EVALUATING THE POSSIBILITY OF TREE SPECIES CLASSIFICATION WITH DUAL-WAVELENGTH ALS DATA

M. Pilarska, W. Ostrowski

Warsaw University of Technology, Faculty of Geodesy and Cartography, Poland - (magdalena.pilarska, wojciech.ostrowski)@pw.edu.pl

Commission II, WG II/3

KEY WORDS: ALS, dual-wavelength, intensity, tree species classification, segmentation

ABSTRACT:

Airborne laser scanning (ALS) plays an important role in spatial data acquisition. One of the advantages of this technique is laser beam penetration through vegetation, which makes it possible to not only obtain data on the tree canopy but also within and under the canopy. In recent years, multi-wavelength airborne laser scanning has been developed. This technique consists of simultaneous acquisition of point clouds in more than one band. The aim of this experiment was to examine and assess the possibilities of tree segmentation and species classification in an urban area. In this experiment, point clouds registered in two wavelengths (532 and 1064 nm) were used for tree segmentation and species classification. The data were acquired with a Riegl VQ-1560i-DW laser scanner over Elblag, Poland, during August 2018. Tree species collected by a botanist team within terrain measurements were used as a reference in the classification process. Within the experiment segmentation and classification process were performed. Regarding the segmentation, TerraScan software and Li et al.'s algorithm, implemented in LidR package were used. Results from both methods are clearly over-segmented in comparison to the manual segments. In Terrasolid segmentation, single reference segments are over-segmented in 28% of cases, whereas, for LidR, over-segmentation occurred in 73% of the segments. According the classification results, Thuja, Salix and Betula were the species, for which the highest classification accuracy was achieved.

1. INTRODUCTION

Airborne laser scanning (ALS) (Baltsavias, 1999) is a well-known and widely used technology. One of the advantages of this technology is fast and accurate data acquisition. ALS technology provides the user with accurate geometric information about registered objects. Point clouds, which are derived from ALS, are mostly used for the generation of digital terrain models (DTMs), digital surface models (DSMs) and in 3D modelling (Hu et al., 2018). Another advantage of ALS is laser beam penetration through vegetation, which not only makes it possible to obtain data on the tree canopy but also within and under the tree. Because of its advantages, ALS is commonly used in forestry (Hyyppä et al., 2012) as well as in urban tree mapping for individual tree segmentation and classification (Zhang et al., 2015), often in fusion with hyperspectral data (Zhang and Qiu, 2014; Alonzo et al., 2014).

Individual tree segmentation often plays a vital role in tree species classification. Segments (a single tree) could just be single objects in object-based image analysis. Another approach utilizes point clouds as a source of geometric features used during tree classification for characterizing single crown structural parameters. For example, Alonzo et al. (2014) proposed 28 ALS-based variables and, after evaluation, used seven of these (five geometrical and two intensity-based variables). Deng et al. (2016) introduced 17 ALS-based features and, after evaluation, chose six of these (five geometrical-based features and average laser intensity for each segment).

ALS is a well-known technology, which has been continuously developed. In recent years, multispectral laser scanning has appeared on the market, aimed at acquiring data in more than one laser wavelength simultaneously. The history of the development of multispectral laser scanners is relatively long (Morsy et al., 2017). The first multispectral laser scanning tests were performed in laboratories using terrestrial laser scanners. In 2011, airborne tests with Riegl scanners were performed. ALS data were initially acquired within three separate flights, utilizing different ALS scanners within each flight (Briese et al., 2012). Such flights should take place within a short time gap because of further integration of the data. Subsequent tests consisted of mounting more than one scanner on an aeroplane (Briese et al., 2013). As a result, two datasets from different sensors were obtained simultaneously. In 2014, the first multispectral laser scanner – Titan – was launched onto the market. Another solution is the Leica Chiroptera 4X, equipped with one bathymetric and one topographic scanner, enabling the acquisition of both bathymetric and topographic data simultaneously.

Intensity derived from light detection and ranging (LiDAR) technology is a relevant feature, which provides information about object properties, e.g., rock properties (Burton et al., 2011). Briese et al. (2013) presented the application of multi-wavelength airborne laser scanning for archaeological prospection. Intensity from multispectral ALS may be used as an additional attribute in point cloud classification (Xiaoliang et al., 2016). Matikainen et al. (2017) proposed application of multispectral airborne laser scanner data for land cover classification and map updating. Tree species classification using multispectral ALS is not a new topic. However, until now, data from a Titan scanner has been used in most experiments presented, meaning that intensity registered in three channels was used (Yu et al., 2017). In Axelsson et al. (2018), multispectral laser scanning data were used for classification of tree species, with an accuracy of 76.5% from the best model.

2. DATA AND STUDY AREA

The data were acquired with a dual-wavelength RIEGL VQ-1560i-DW. This laser scanner offers two channels of differing wavelengths: green (532 nm) and infrared (1064 nm). Both channels provide straight, parallel scan lines. The scan lines of the two channels are tilted against each other by 28 degrees (Riegl). The scanner provides two separate point clouds: one registering intensity in green wavelengths and the other in infrared. This laser scanner has successfully identified possible applications in agriculture and vegetation mapping. Intensity registered in two wavelengths enables calculation of the Green Normalized Difference Vegetation Index (GNDVI).

Data were obtained in an urban area over Elblag, Poland, in August 2018. The mean density of the point cloud was 12 points/m^2. In Table 1 number of training and classified trees from selected species collected by a botanist team is presented.

Species	No of training trees	No of classified trees
Thuja	16	14
Salix	10	11
Picea	16	26
Robinia	17	19
Tilia	26	50
Acer	20	35
Aesculus	15	14
Sorbus	16	17
Crataegus	13	14
Quercus	7	7
Ulmus	14	15
Betula	13	14
Total	183	236

Table 1. Number of training and classified trees from selected species

3. METHODOLOGY

The dual-wavelength data were pre-processed. For both channels, there was one point cloud, so the datasets had to be integrated. This was done in such a way that every echo from one point cloud had an additional attribute (intensity) from the nearest neighbour of the second point cloud. As a result, every echo had two intensity values in two channels: green and infrared. The next step performed was segmentation. Single trees from different species were delineated. Points from the high and medium classes of vegetation were then assigned to the segment. Points in every segment statistic for both channels were calculated. These statistics were: min., max., mean, median, standard deviation, root mean square (RMS), sigma and skewness describing the symmetry of the sample. These statistics were calculated for both channels and used as input features in the classification process.

As a first step, histograms for all tree species were generated. The histograms were generated for first echoes from classes four to five (medium and high vegetation) for two attributes: intensity in infrared and green wavelengths. The histograms may indicate which species are resembled and might lead to difficulties in distinguishing the tree species. Thus, it may be necessary to combine some species into one group during the classification process. Tree species obtained from terrain vision by biologists served as a reference in the classification process.

Classification was performed using a Matlab program and the Classification Learner application. All classification algorithms were tested and the most accurate model was chosen. At the outset, all tree species were used for training: Thuja, Salix, Ulmus, Picea, Robinia, Tilia, Acer, Aesculus, Sorbus, Crataegus, Betula and Quercus. In subsequent steps, the species were combined into groups. After species combining, the model training process was carried out and this was stopped at the point when significant increases in accuracy were no longer observed. The model that included the most species was chosen for further classification.

Geometric features of single trees were derived from point clouds segmented based on geometric relationships between points. Segmentation was performed only for points from the high vegetation class, with two different approaches (both based on point clouds). The first method was watershed segmentation, implemented in Terrasolid software as a grouping method, with only two parameters: minimum height of tree (2m) and minimum number of points in a group/segment (20). The second method used was the algorithm developed by Li et al. (2012), implemented using the LidR package (Airborne LiDAR Data Manipulation and Visualization for Forestry). Six different parameters are available, but we decided to set it all to default values.

Two classification approaches are presented in this article. In the first approach, the classification process focused on amplitude in green and infrared bands. In the second approach, amplitude in the infrared channel and GNDVI were used to classify the tree species. The GNDVI has a value from –1 to 1 and is calculated according to the formula (1):

$$\mathrm{GNDVI} = \frac{(\mathrm{NIR}-\mathrm{G})}{(\mathrm{NIR}+\mathrm{G})} \tag{1}$$

Where NIR – intensity in infrared channel
G – intensity in green channel

4. RESULTS

In this section, results of the performed classification are described. To begin with, histograms of amplitude in infrared and green wavelengths are presented.

4.1 Histograms

Table 2 presents histograms of the amplitude in infrared and green wavelengths. According to the histograms, it can be seen that the distribution of amplitude values among some species (particularly Tilia and Acer) are very similar to each other. This may make it difficult (or almost impossible) to distinguish these species from one another. Thus, it may be necessary to combine some species into one group during the classification process. On the other hand, histograms presenting infrared amplitude distribution are different for Salix and Betula in comparison to other species.

4.2 Segmentation results

Both segmentation methods resulted in a point cloud with an additional attribute integer (TreeID or Group), indicating which points belong to a single segment. As a reference, manual crown delineation data were used. The extent of each tree was estimated from CHM and point cloud data collected in August. An additional data source was also used for interpretation, consisting of filed measurements and leaf-off point clouds from February. Results from both methods are clearly over-segmented (Fig. 1). For 376 reference segments, watershed segmentation in Terrasolid created 442 groups. When Li et al.'s algorithm (2012) was implemented in LidR, it created 1122 trees

https://doi.org/10.5194/isprs-archives-XLII-2-W13-1097-2019 | © Authors 2019. CC BY 4.0 License.

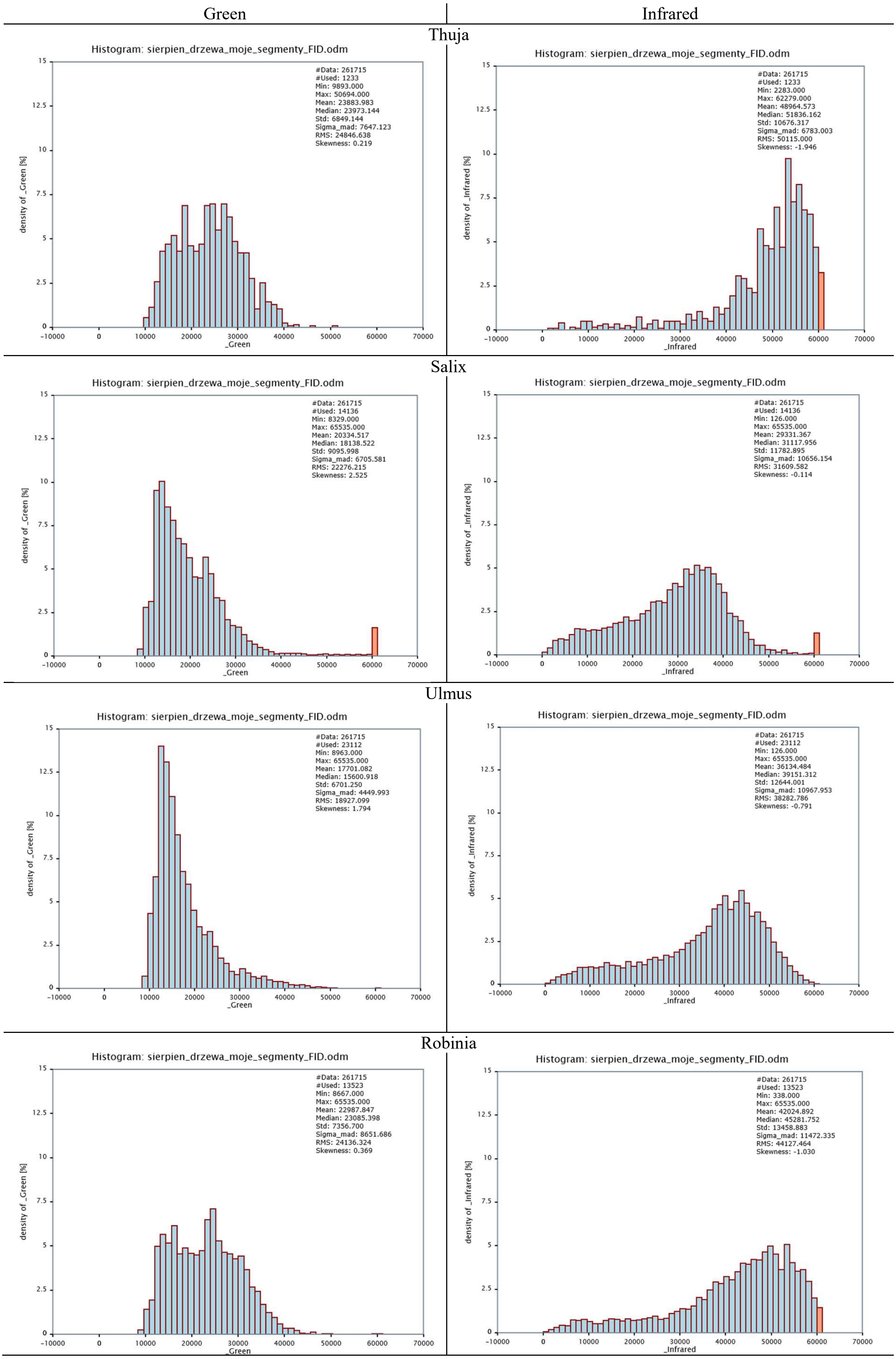
Green
Infrared
Thuja
Histogram: sierpien_drzewa_moje_segmenty_FID.odm
#Data: 261715
#Used: 1233
Min: 9893.000
Max: 50694.000
Mean: 23883.983
Median: 23973.144
Std: 6849.144
Sigma_mad: 7647.123
RMS: 24846.638
Skewness: 0.219
density of _Green [%]
_Green
Histogram: sierpien_drzewa_moje_segmenty_FID.odm
#Data: 261715
#Used: 1233
Min: 2283.000
Max: 62279.000
Mean: 48964.573
Median: 51836.162
Std: 10676.317
Sigma_mad: 6783.003
RMS: 50115.000
Skewness: -1.946
density of _Infrared [%]
_Infrared
Salix
Histogram: sierpien_drzewa_moje_segmenty_FID.odm
#Data: 261715
#Used: 14136
Min: 8329.000
Max: 65535.000
Mean: 20334.517
Median: 18138.522
Std: 9095.998
Sigma_mad: 6705.581
RMS: 22276.215
Skewness: 2.525
density of _Green [%]
_Green
Histogram: sierpien_drzewa_moje_segmenty_FID.odm
#Data: 261715
#Used: 14136
Min: 126.000
Max: 65535.000
Mean: 29331.367
Median: 31117.956
Std: 11782.895
Sigma_mad: 10656.154
RMS: 31609.582
Skewness: -0.114
density of _Infrared [%]
_Infrared
Ulmus
Histogram: sierpien_drzewa_moje_segmenty_FID.odm
#Data: 261715
#Used: 23112
Min: 8963.000
Max: 65535.000
Mean: 17701.082
Median: 15600.918
Std: 6701.250
Sigma_mad: 4449.993
RMS: 18927.099
Skewness: 1.794
density of _Green [%]
_Green
Histogram: sierpien_drzewa_moje_segmenty_FID.odm
#Data: 261715
#Used: 23112
Min: 126.000
Max: 65535.000
Mean: 36134.484
Median: 39151.312
Std: 12644.001
Sigma_mad: 10967.953
RMS: 38282.786
Skewness: -0.791
density of _Infrared [%]
_Infrared
Robinia
Histogram: sierpien_drzewa_moje_segmenty_FID.odm
#Data: 261715
#Used: 13523
Min: 8667.000
Max: 65535.000
Mean: 22987.847
Median: 23085.398
Std: 7356.700
Sigma_mad: 8651.686
RMS: 24136.324
Skewness: 0.369
density of _Green [%]
_Green
Histogram: sierpien_drzewa_moje_segmenty_FID.odm
#Data: 261715
#Used: 13523
Min: 338.000
Max: 65535.000
Mean: 42024.892
Median: 45281.752
Std: 13458.883
Sigma_mad: 11472.335
RMS: 44127.464
Skewness: -1.030
density of _Infrared [%]
_Infrared

Green	Infrared

Tilia

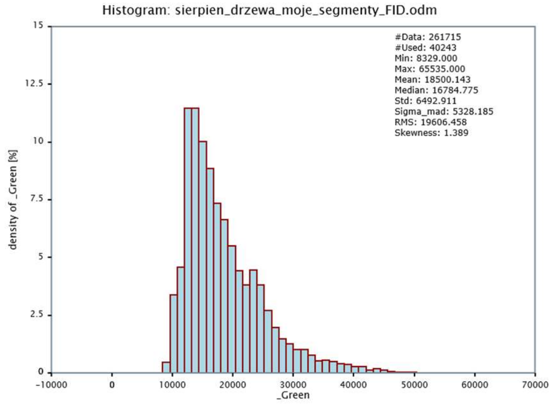

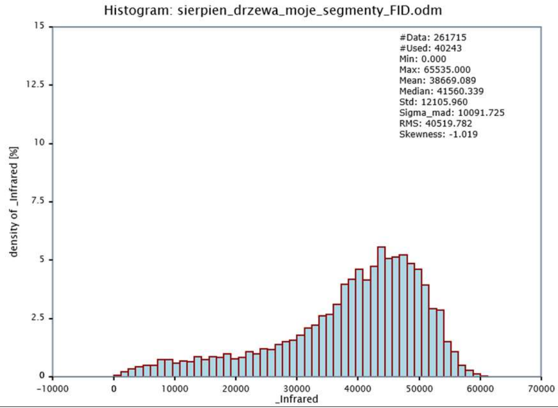

Acer

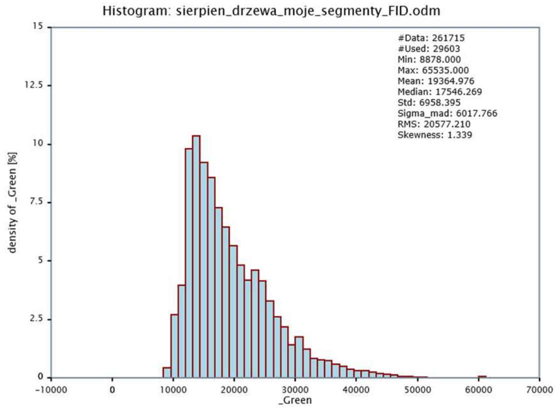

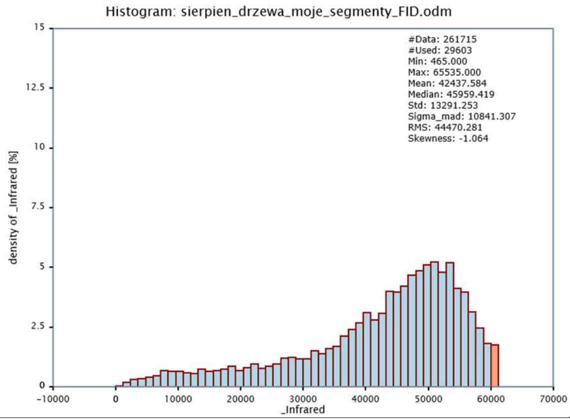

Quercus

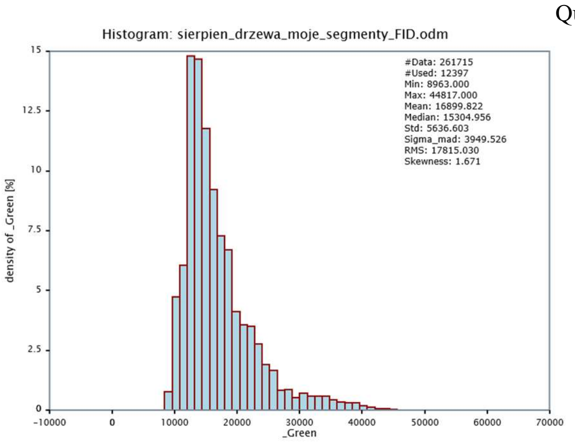

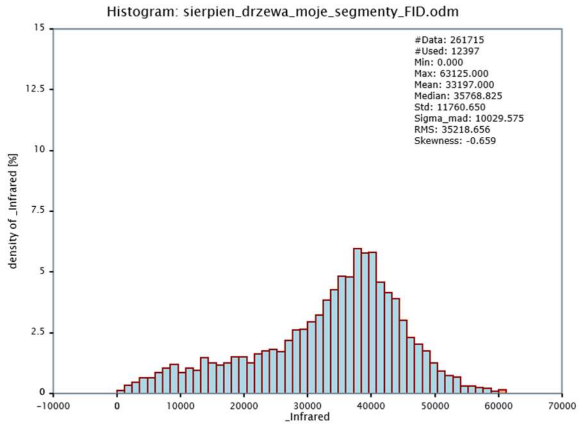

Betula

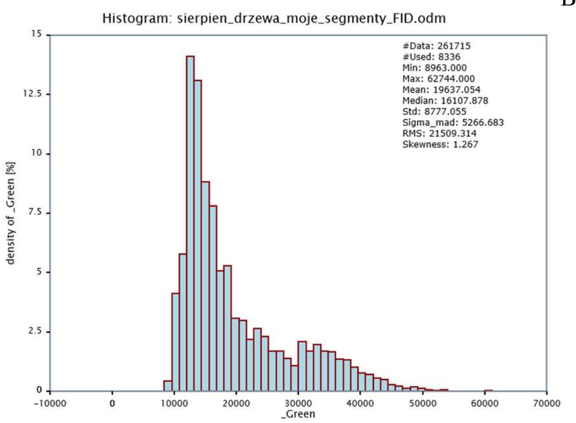

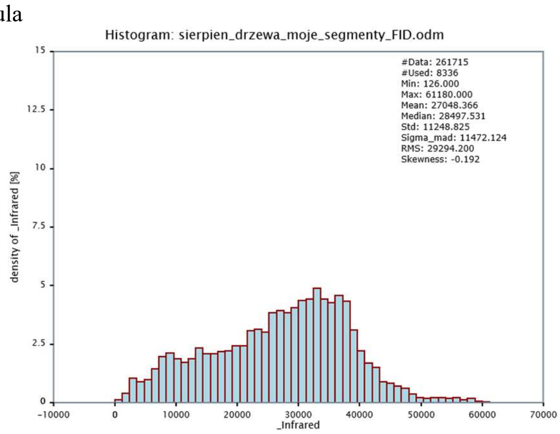

Table 2. Histograms presenting intensity for selected tree species in green and infrared channel

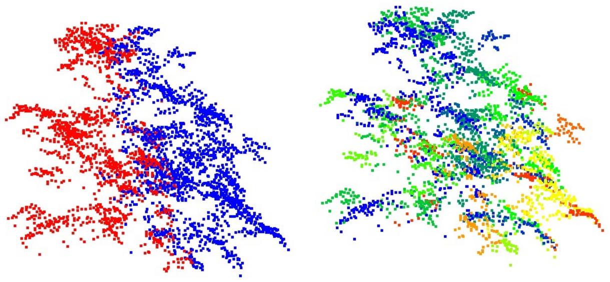

Figure 1. Example of segmentation result. The results for both algorisms are clearly over-segmented. Single reference trees are divided into two segments by Terrasolid (left) and into several segments by LidR (right).

In the case of over-segmentation, single reference trees are divided into several segments. In the results of Terrasolid segmentation, single reference segments are over-segmented in 28% of cases, whereas, for LidR, over-segmentation occurred in 73% of the segments (more details of these results are summarized in Table 3). When the negative influence of over-segmentation is mostly connected with corruption of the geometrical features values, under-segmentation (when resulting segments are within more than just a single reference segment) can have an even more devastating influence on the classification results. The results of Terrasolid segmentation show under-segmentation in 20% of the segments and in 11.6% of the LidR results (more detailed results are summarized in Table 4).

Presented results proved that tree segmentation is topic, which still may be explored. Because the results of individual tree crown segmentation and delineation are far below the authors' expectations, the authors decided not to use geometrical features in the final experiments and classification, thereby avoiding the classification results being biased by erroneous segmentation. For intensity-based classification, only reference segments were used.

No of resulted segments in single reference segment	0	**1**	2	3	4	5	6	7 - 22
LidR	6	**94**	79	59	46	24	24	44
TerraSolid	6	**246**	84	3	8	1	1	0

Table 3. Segmentation accuracy: the number of resulted segments that are within the single reference segment (over-segmentation).

Number of reference segments in single result segment	5	4	3	2	**1**
LidR	0	1	9	120	**992**
TerraSolid	1	3	8	76	**354**

Table 4 Segmentation accuracy: the number of reference segments that are within the single result segment (under-segmentation).

4.3 Classification results

As a first step, all 12 species were used. All classifiers in the Classification Learner application were tested. The best results were given by SVM classifier; therefore, this classifier was chosen for subsequent steps.

To start with, all features for two channels (min., max., median, mean, sigma, standard deviation, RMS and skewness) were used in the classifier training. The accuracy of the classifier was 52.5%. Other assorted combinations of features were used in order to assess their importance in SVM classification. Min., max., mean, standard deviation, RMS and skewness features gave the highest accuracy of 55.7%, i.e., 3.2 percentage points more in comparison to the approach where all features were included.

<table>
<tr><th rowspan="2">Species</th><th colspan="4">Accuracy [%]</th></tr>
<tr><th>12 classes</th><th>9 classes</th><th>8 classes</th><th>6 classes</th></tr>
<tr><td>Thuja</td><td>100</td><td>92.9</td><td>92.9</td><td>92.9</td></tr>
<tr><td>Salix</td><td>81.8</td><td>81.8</td><td>81.8</td><td>72.7</td></tr>
<tr><td>Picea</td><td>42.3</td><td>42.3</td><td>46.2</td><td>34.6</td></tr>
<tr><td>Robinia</td><td>63.2</td><td>47.4</td><td>42.1</td><td>42.1</td></tr>
<tr><td>Tilia cordata Mill</td><td>28.0</td><td rowspan="3">69.7</td><td rowspan="4">81.9</td><td rowspan="7">87.5</td></tr>
<tr><td>Acer</td><td>31.4</td></tr>
<tr><td>Aesculus</td><td>57.1</td></tr>
<tr><td>Sorbus</td><td>29.4</td><td>17.6</td></tr>
<tr><td>Crataegus</td><td>35.7</td><td>35.7</td><td>28.6</td></tr>
<tr><td>Quercus</td><td>0</td><td rowspan="2">31.8</td><td rowspan="2">22.7</td></tr>
<tr><td>Ulmus</td><td>13.3</td></tr>
<tr><td>Betula</td><td>85.7</td><td>85.7</td><td>85.7</td><td>78.6</td></tr>
<tr><td>Total accuracy</td><td>43.6</td><td>58.1</td><td>66.9</td><td>77.1</td></tr>
<tr><td>Model accuracy</td><td>55.7</td><td>66.1</td><td>70.5</td><td>78.1</td></tr>
</table>

Table 5. Results of tree species classification using green and infrared intensity

In Table 5, the results of all the classification processes are presented. All tree species were classified initially. The results show which classes can be distinguished from one another. For example, Thuja, Salix, Robinia, Aesculus and Betula are characterized by a classification accuracy higher than 50%. Moreover, the accuracy of Thuja, Salix and Betula classifications was higher than 80%. However, the total accuracy of all trees was lower than 50%, thus some species were combined into groups. This integration was performed after analysis of the confusion matrix. As a first step, Quercus and Ulmus were assigned to one group, and Tilia, Acer and Aesculus were assigned to another group. The model accuracy increased to 66.1%, and the total classification accuracy was 58.1%. After combining the species into groups, the classification accuracy of the models was found to increase.

The second approach involved using GNDVI and infrared channel amplitude in the classification process. This approach was almost the same as in the green-infrared classification. The results of the classification are presented in Table 6.

According to Table 6, it can be noted that the results obtained are similar to those from the first approach. The same species (i.e., Thuja, Salix and Betula) are easy to distinguish. For Thuja, the same accuracy was achieved in both approaches (92.9%). For Salix, higher accuracy was achieved in the second approach (90.9%), compared to the first one (72.7%). Similar results were obtained for Betula (78.6% correctly classified trees in the first approach and 85.7% in the second one).

https://doi.org/10.5194/isprs-archives-XLII-2-W13-1097-2019

<table>
<tr><th rowspan="2">Species</th><th colspan="3">Accuracy [%]</th></tr>
<tr><th>12 classes</th><th>9 classes</th><th>7 classes</th></tr>
<tr><td>Thuja</td><td>92.9</td><td>100</td><td>92.9</td></tr>
<tr><td>Salix</td><td>90.0</td><td>63.6</td><td>90.9</td></tr>
<tr><td>Picea</td><td>26.9</td><td>23.1</td><td>30.8</td></tr>
<tr><td>Robinia</td><td>68.4</td><td>63.2</td><td>47.4</td></tr>
<tr><td>Tilia cordata Mill</td><td>34.0</td><td>34</td><td rowspan="6">87.6</td></tr>
<tr><td>Acer</td><td>28.6</td><td rowspan="4">56.3</td></tr>
<tr><td>Aesculus</td><td>64.3</td></tr>
<tr><td>Quercus</td><td>0</td></tr>
<tr><td>Ulmus</td><td>26.7</td></tr>
<tr><td>Sorbus</td><td>41.2</td><td>23.5</td></tr>
<tr><td>Crataegus</td><td>21.4</td><td>35.7</td><td>14.3</td></tr>
<tr><td>c</td><td>78.6</td><td>71.4</td><td>85.7</td></tr>
<tr><td>Total accuracy</td><td>44.1</td><td>48.7</td><td>73.7</td></tr>
<tr><td>Model accuracy</td><td>55.7</td><td>60.4</td><td>76.5</td></tr>
</table>

Table 6. Results of tree species classification using GNDVI and infrared intensity

5. CONCLUSIONS

In the presented experiment, dual-wavelength ALS data were used in the classification of tree species. Two approaches were examined: using intensity registered in a green and an infrared channel, and using infrared and GNDVI values for classification. The results for both approaches were similar, i.e., the highest classification accuracy was achieved for Thuja, Salix and Betula. Higher accuracy for these species was obtained in the second classification approach. For Thuja, 92.9% of trees were correctly classified and the accuracy for Salix and Betula were 90.9% and 78.6%, respectively. According to other species, the classification accuracy was much lower. However, Robinia also achieved almost 70% accuracy.

In segmentation process TerraScan software and Li et al.'s algorithm, implemented in LidR package were used. Results derived from both methods are noticeably over-segmented in comparison to the manual segmentation. In Terrasolid segmentation, single reference segments are over-segmented in 28% of cases, whereas, for LidR, over-segmentation occurred in 73% of the segments. The segmentation results were unsatisfactory for the authors, so it was decided not to use the geometric features of the segments in tree species classification. Additionally, the results proved that single tree segmentation from ALS may be still explored.

Analysis of the classification results reveals that intensity is a valuable source of information about trees. However, few can be distinguished reliably. In this experiment, only radiometric information was used. In further analysis, geometric features should be also included, which may increase the classification accuracy of species with similar radiometric properties.

ACKNOWLEDGEMENTS

The authors would like to thank the OPEGIEKA Sp. z o. o. company for providing the data.

REFERENCES

Alonzo, M., Bookhagen, B., Roberts, D.A., 2014. Urban tree species mapping using hyperspectral and lidar data fusion. Remote Sensing of Environment, 148, 70-83. http://dx.doi.org/10.1016/j.rse.2014.03.018.

Axelsson, A., Lindberg, E., Olsson, H., 2018. Exploring Multispectral ALS Data for Tree Species Classification. *Remote Sensing*, 10(2), 183. https://doi.org/10.3390/rs10020183.

Baltsavias, E. P., 1999. Airborne laser scanning: basic relations and formulas. *ISPRS Journal of photogrammetry and remote sensing*, 54(2-3), 199-214. https://doi.org/10.1016/S0924-2716(99)00015-5.

Briese, C., Pfennigbauer, M., Lehner, H., Ullrich, A., Wagner, W., Pfeifer, N., 2012. Radiometric calibration of multi-wavelength airborne laser scanning data. *ISPRS Ann. Photogramm. Remote Sens. Spat. Inf. Sci*, 1, 335-340. https://doi.org/10.5194/isprsannals-I-7-335-2012, 2012.

Briese, C., Pfennigbauer, M., Ullrich, A., Doneus, M., 2013. Multi-wavelength airborne laser scanning for archaeological prospection. *Int. Arch. Photogramm. Remote Sens. Spat. Inf. Sci*, 40, 119-124. https://doi.org/10.5194/isprsarchives-XL-5-W2-119-2013.

Burton, D., Dunlap, D. B., Wood, L. J., Flaig, P. P., 2011. Lidar intensity as a remote sensor of rock properties. *Journal of Sedimentary Research*, 81(5), 339-347. https://doi.org/10.2110/jsr.2011.31.

Deng, S., Katoh, M., Yu, X., Hyyppä, J., Gao, T., 2016. Comparison of tree species classifications at the individual tree level by combining ALS data and RGB images using different algorithms. *Remote Sensing*, 8(12), 1034. https://doi.org/10.3390/rs8121034.

Hu, P., Yang, B., Dong, Z., Yuan, P., Huang, R., Fan, H., Sun, X., 2018. Towards Reconstructing 3D Buildings from ALS Data Based on Gestalt Laws. *Remote Sensing*, 10(7), 1127. https://doi.org/10.3390/rs10071127.

Hyyppä, J., Holopainen, M., Olsson, H., 2012. Laser Scanning in Forests. *Remote Sensing*, 4(10), pp.2919–2922. https://doi.org/10.3390/rs4102919.

Li, W., Guo, Q., Jakubowski, M., Kelly, M., (2012. A New Method for Segmenting Individual Trees from the Lidar Point Cloud. *Photogrammetric Engineering & Remote Sensing*, 78(1), pp.75–84. https://doi.org/10.14358/PERS.78.1.75.

Matikainen, L., Karila, K., Hyyppä, J., Litkey, P., Puttonen, E., Ahokas, E., 2017. Object-based analysis of multispectral airborne laser scanner data for land cover classification and map updating. *ISPRS Journal of Photogrammetry and Remote Sensing*, 128, 298-313. https://doi.org/10.1016/j.isprsjprs.2017.04.005.

Morsy, S., Shaker, A., El-Rabbany, A., 2017. Multispectral LiDAR data for land cover classification of urban areas. *Sensors*, 17(5), 958. https://doi.org/10.3390/s17050958.

Riegl: http://www.riegl.com/nc/products/airborne-scanning/produktdetail/product/scanner/55/. Access: 02.04.2019

Xiaoliang, Z. O. U., Guihua, Z. H. A. O., Jonathan, L. I., Yuanxi, Y. A. N. G., Yong, F. A. N. G., 2016. 3D land cover classification based on multispectral lidar point clouds. *International Archives of the Photogrammetry, Remote Sensing & Spatial Information Sciences*, 41, 741-747. https://doi.org/10.5194/isprs-archives-XLI-B1-741-2016.

Yu, X., Hyyppä, J., Litkey, P., Kaartinen, H., Vastaranta, M., Holopainen, M., 2017. Single-Sensor Solution to Tree Species Classification Using Multispectral Airborne Laser Scanning. *Remote Sensing*, 9(2), 108. https://doi.org/10.3390/rs9020108.

Zhang C., Qiu F., 2012. Mapping Individual Tree Species in an Urban Forest Using Airborne Lidar Data and Hyperspectral Imagery. *Photogrammetric Engineering & Remote Sensing*, 78(10), pp.1079–1087.
https://doi.org/10.14358/PERS.78.10.1079.

Zhang, C., Zhou, Y., Qiu, F., 2015. Individual Tree Segmentation from LiDAR Point Clouds for Urban Forest Inventory. Remote Sensing, 7(6), pp.7892–7913.
https://doi.org/10.3390/rs70607892.